

A CALCULATION PROCEDURE FOR THREE-DIMENSIONAL TURBULENT FLOWS USING NON-STAGGERED GRIDS

SONG Baojun, GU Chuangang and MIAO Yongmiao

Dept of Power Machinery Engineering, Xian Jiaotong University
 Xian, Shaanxi 710049, P R CHINA

Abstract

A calculation procedure is developed for three-dimensional incompressible, steady Navier-Stokes equations in general curvilinear coordinate system by using non-staggered grids. A momentum interpolation is applied to eliminate the oscillation of pressure and velocity. Through the numerical computation on the laminar flow in a square duct, it is proved that the convergency and the precision of the present procedure are satisfactory. Finally, the three-dimensional turbulent flows are numerically computed in a radial rotating duct and a volute with trapezoid cross-section. The computed results are compared with the available experimental data.

Notation

A	= coefficients in the general finite difference equations
B	= width of the rotating duct
B_{ij}	= coefficient matrix in Eq. (6)
C_{ij}	= coefficient matrix in Eq. (7)
C_r, C_θ	= velocity components in r and θ directions, respectively
G^Φ	= effective diffusion coefficient for the general scalar Φ
H	= height of the rotating duct
J	= Jacobian of the transformation
L	= length of the rotating duct
M_1, M_2, M_ξ	= convective terms along the (ξ, η, ζ) directions, respectively
p	= pressure
p'	= pressure correction
r, θ , z	= cylindrical coordinates
Re	= Reynolds number
S^Φ	= source term in the finite difference equation for the general scalar Φ
u, v, w	= Cartesian velocity components
u_m	= cross-sectional average velocity
x, y, z	= Cartesian coordinates
ξ, η, ζ	= curvilinear coordinates
ρ	= density
$\Delta\xi, \Delta\eta, \Delta\zeta$	= cell boundary sizes in ξ, η and ζ directions in the transformed plane

Ω = angular velocity of the rotating duct.

Φ = general scalar quantity

Subscript

ξ, η, ζ = differentiation with respect to these variables

Introduction

In practice, there exist many of three-dimensional turbulent flows in complex passages. The present numerical computation for fluid flows follows essentially SIMPLE method (Caretto, et al., 1972). However, this method suffers severely from geometric limitation when it is used to calculate the flows in complex passages. There are other attempts to be developed numerical techniques using the curvilinear coordinates. Demirdzic, et al. (1980) developed a finite volume method, which is applied to calculate the flowfield inside the general passages. In this method, the governing equations are represented according to arbitrary contravariant velocity components. However, since the semistrong conservation form of the governing equations is used, the convergency of the numerical method becomes poor. In addition, since the staggered grid arrangements are used to eliminate the oscillation of pressure and velocity, a lot of interpolation computations are required in each step. With the aim of overcoming the drawback of the staggered grid technique, Rhie and Chow (1983) presented a numerical scheme in which non-staggered grid technique was used and the governing equations of Cartesian components were solved.

In the present paper, a calculation procedure is developed for three-dimensional turbulent flows in complex passages by using the non-staggered grids. A momentum interpolation is applied to eliminate the oscillation of pressure and velocity. The laminar flow inside a square duct is calculated to discuss the accuracy and convergency of the present procedure. The three-dimensional flows are numerically computed in a radial rotating duct and a volute with trapezoid cross-section.

Governing Equations

For steady flow, the governing equations involving the continuity, momentum and other scalars are written as following common form.

$$\text{div}(\rho \vec{U} \cdot \Phi - G^\phi \cdot \text{grad} \Phi) = S^\phi \quad (1)$$

where Φ is an arbitrary variable, \vec{U} the mean velocity vector, G^ϕ an effective diffusion coefficient and S^ϕ the source term. According to the transformation $\xi = \xi(x, y, z)$, $\eta = \eta(x, y, z)$ and $\zeta = \zeta(x, y, z)$, Eq. (1) can be transformed into the new form in the (ξ, η, ζ) coordinates. That is,

$$\begin{aligned} & \frac{1}{J} \left[\frac{\partial}{\partial \xi} (\rho M_1 \Phi) + \frac{\partial}{\partial \eta} (\rho M_2 \Phi) + \frac{\partial}{\partial \zeta} (\rho M_3 \Phi) \right] \\ &= \frac{1}{J} \left\{ \frac{\partial}{\partial \xi} \left[\frac{G^\phi}{J} (j_{11} \Phi_\xi + j_{21} \Phi_\eta + j_{31} \Phi_\zeta) \right] \right. \\ &+ \frac{\partial}{\partial \eta} \left[\frac{G^\phi}{J} (j_{12} \Phi_\xi + j_{12} \Phi_\eta + j_{32} \Phi_\zeta) \right] \\ &+ \left. \frac{\partial}{\partial \zeta} \left[\frac{G^\phi}{J} (j_{13} \Phi_\xi + j_{23} \Phi_\eta + j_{33} \Phi_\zeta) \right] \right\} + S^\phi \quad (2) \end{aligned}$$

where J is Jacobian of the transformation, and

$$M_i = j_{1i} u + j_{2i} v + j_{3i} w \quad (i = 1, 2, 3) \quad (3)$$

where $j_{11} \sim j_{33}$ and $j_{1i} \sim j_{3i}$ are the coefficients of coordinate transformation. They are determined from x_i , x_{ij} , etc. (Song, 1990)

For turbulent flow, the diffusion coefficient in the momentum equations is replaced with an effective viscosity μ_{eff} , which is the combination of molecular and turbulent viscosity. The turbulent viscosity is determined from the values of the turbulence kinetic energy and its dissipation rate. And the values of turbulent kinetic energy and its dissipation rate are determined from their own transport equations (Launder and Spalding, 1974).

Numerical Procedure

Computational domain is discretized in terms of non-

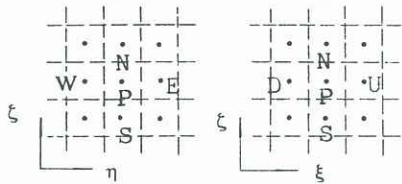


Fig.1 Grid arrangements in computational domain

staggered grid arrangements (Fig. 1). In terms of the SIMPLE procedure, the difference equation for Eq. (2) is obtained as follows;

$$\begin{aligned} A_P \Phi_P &= A_E \Phi_E + A_W \Phi_W + A_N \Phi_N + A_S \Phi_S + A_U \Phi_U + A_D \Phi_D \\ &+ S^\phi J A \xi A \eta A \zeta + S^\phi J A \xi A \eta A \zeta \quad (4) \end{aligned}$$

where the coefficients A involve the flow properties of convection, diffusion, area, etc. They are modified by employing the hybrid scheme. S^ϕ is originated from the cross derivatives in the diffusion terms and is the result of the nonorthogonal coordinate system. For convenient sake, S^ϕ is combined with S^ϕ in the following equations. In equation (4), it is assumed that Φ is equal to u , v and w respectively, and the discretized equations of the momentum equations can be obtained.

The linkage between the momentum and continuity equations is handled through a pressure-correction equation (Patankar, 1980). It is assumed that velocity components

are u^* , v^* and w^* when pressure field is p^* . They should satisfy the discretized momentum equations. In general, u^* , v^* and w^* do not satisfy the continuity equation. It is assumed that p^* is corrected according to

$$p = p^* + p' \quad (5)$$

Then, the velocity components will be corrected by the relations

$$\begin{aligned} u &= u^* + B_{11} p'_\xi + B_{12} p'_\eta + B_{13} p'_\zeta \\ v &= v^* + B_{21} p'_\xi + B_{22} p'_\eta + B_{23} p'_\zeta \\ w &= w^* + B_{31} p'_\xi + B_{32} p'_\eta + B_{33} p'_\zeta \end{aligned} \quad (6)$$

And the correction equations for M_1, M_2 and M_3 are obtained from Eq. (3), that is,

$$M_i = M_i^* + C_{1i} p'_\xi + C_{2i} p'_\eta + C_{3i} p'_\zeta \quad (i = 1, 2, 3) \quad (7)$$

where M_i^* is based on u^* , v^* and w^* . $C_{11} - C_{33}$ are coefficients involving B_{ij}, j_{ij} . Substituting Eq. (7) into the discretized continuity equation, and then using the second-order center-difference approximations for the pressure gradients on the control volume surface, one obtains the pressure correction equation, that is,

$$A_P p'_P = A_E^p p'_E + A_W^p p'_W + A_N^p p'_N + A_S^p p'_S + A_U^p p'_U + A_D^p p'_D + S^p \quad (8)$$

where the coefficients A^p involve coefficients B_{ij}, C_{ij} , density, etc., and S^p represents the imbalance of mass in a control volume and the added source terms resulting from the nonorthogonal coordinate system.

Since the non-staggered grids are used, the oscillation of pressure and velocity is produced (Patankar, 1980). To eliminate the oscillation, the momentum interpolation equations are applied. In the computational domain (shown in Fig. 1), the u -momentum equation at the grid node (i, j, k) (node P) is written as follows;

$$u_{i,j,k} = H_{i,j,k}^u + (B_{11} p'_\xi)_{i,j,k} \quad (9)$$

where H represents the combination of the momentum terms, source terms and the pressure gradients along η and ζ directions. In similar manner, u -momentum equations in the grid node $(i+1, j, k)$ and in the control volume surface $(i+1/2, j, k)$ are written as follows;

$$u_{i+1,j,k} = H_{i+1,j,k}^u + (B_{11} p'_\xi)_{i+1,j,k} \quad (10)$$

$$u_{(i+1/2,j,k)} = H_{(i+1/2,j,k)}^u + (B_{11} p'_\xi)_{(i+1/2,j,k)} \quad (11)$$

where $(i+1/2, j, k)$ denotes the intersection of the control volume surface and gridline. Similarly, the v -momentum and w -momentum equations in $(i+1/2, j, k)$ are also obtained. Substituting (11) into (3), one can obtain the convective term along the ξ direction in control volume surface, i. e.,

$$M_1 = \bar{M}_{(i+1/2,j,k)} + (\bar{B} p'_\xi)_{(i+1/2,j,k)} \quad (12)$$

where $\bar{M}_{(i+1/2,j,k)} = \bar{j}_{11} H_{(i+1/2,j,k)}^u + \bar{j}_{21} H_{(i+1/2,j,k)}^v + \bar{j}_{31} H_{(i+1/2,j,k)}^w$, H^u, H^v and H^w in $(i+1/2, j, k)$ are determined from the linear interpolation of H^u, H^v and H^w in (i, j, k) and $(i+1, j, k)$, and H^u in (i, j, k) can be determined from Eq. (9) in terms of the preliminary values of velocity and pressure.

From the equation (12), it is seen that the flux on the control volume surface is related with the pressure in the neighbouring nodes.

The main calculation steps in the present procedure are

as follows;

- (1) The pressure field is assigned guessed values
- (2) The momentum equations are solved, the convective terms involving in the coefficients in the equations being evaluated in terms of Eq. (12).
- (3) the pressure correction equation is solved, and then the pressure and velocity are corrected
- (4) The kinetic energy and its dissipation rate equations are solved so as to provide the new distribution of effective viscosity.
- (5) Steps 2,3 and 4 are repeated until a converged solution is obtained

Results

Laminar Flow in a Square Duct. In order to validate the present procedure, the laminar entrance flow in a square duct is numerically studied. Fig. 2 shows the comparison of the main-stream velocity along the centerline. It is evident that the number of grid nodes have a great influence on the precisions of solution. the computations are performed in MICRO VAX II.

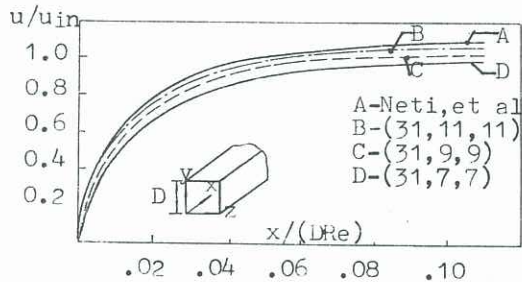


Fig.2 Development of main-stream velocity along centerline

Turbulent Flow in A Radial Rotating Duct Fig. 3 shows a channel rotating about an axis normal to the main flow direction. The Cartesian and curvilinear coordinates rotating about the axis are chosen to facilitate the calculation. Coriolis and centrifugal forces must be included in the momentum equations but not in the $k-\epsilon$ equations.

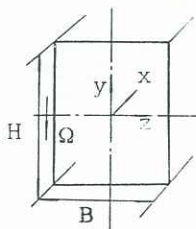


Fig.3 Coordinates of rotating duct

The geometrical dimensions and flow parameters are as follows;

$$H=44.5\text{mm}, B=121\text{mm}, L=610\text{mm}, \\ u_m=15.2\text{m/s}, \Omega=300\text{rpm}, \text{Re}=66500$$

In the calculation, a uniform velocity at the entrance is assumed with no secondary velocities. At the outlet plane, the main stream velocity is first estimated from the upstream value and then is adjusted to satisfy the total mass flow

given, and the gradients of other variables along the main flow direction are assumed zero.

The computed data are compared at 610mm with measured main stream velocities in Fig. 4 and cross-velocities in Fig. 5. The predictions are satisfactory.

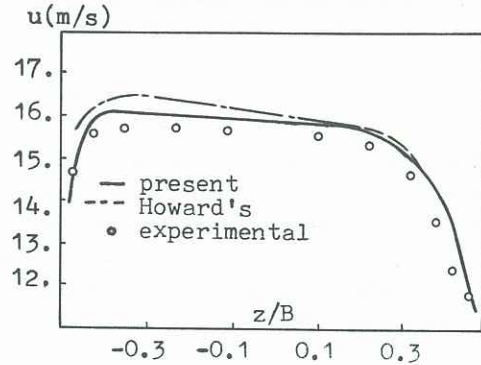


Fig.4 Main-stream velocity distribution (x=610mm, y=0)

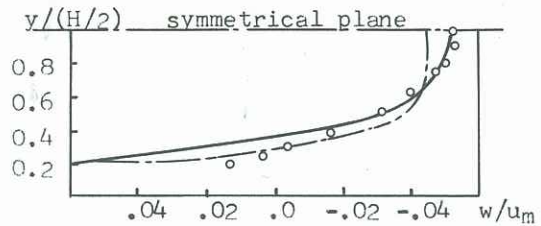


Fig.5 Secondary velocity distribution (x=610mm, z=0)

Turbulent Flow in A Volute with Trapezoid. A schematic diagram of a volute is shown in Fig. 6. The geometrical dimensions and flow parameters are as follows

$$D_2=480\text{mm}, D_4=538\text{mm}, b_1=64\text{mm} \\ \varphi=60^\circ, Q=96\text{m}^3/\text{min}$$

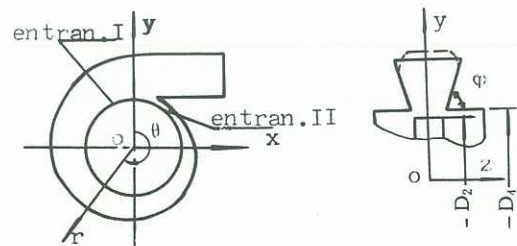


Fig.6 Volute geometry and coordinates

The outer wall of the volute is a section of spiral, which is designed according to the one-dimensional inviscid theory. With the reference to Fig. 6, based on the cylindrical coordinates (r, θ, z) , the curvilinear coordinates (ξ, η, ζ) may be expressed by

$$\xi = C_\xi \cdot \theta \\ \eta = C_\eta \cdot \frac{r - r_i}{r_0 - r_i} \\ \zeta = C_\zeta \cdot \frac{z}{z_0 - z_i}$$

where r_i is the inner radius of the volute, and it is constant; r_o is the outer radius, and it changes with θ ; $(z_0 - z_i)$ is the width of the trapezoid cross-section, and it changes with θ and r ; C_1, C_2 and C_3 are transformation constants.

With reference to Fig. 6, The computation domain is bounded by the first entrance (Entrance I), the second entrance (Entrance II), walls and exit plane. At the entrance I, C_r, C_θ are given, C_z is set to zero. At the entrance II, C_r, C_z are set to zero, C_θ is given in terms of the one-dimensional inviscid theory. At the exit plane, the distribution of main flow velocity is first estimated and then is adjusted to give the required mass flow. Also, the gradients of other variables along the main flow direction are assumed zero. Close to the wall, all the transport processes are modelled by using the wall function method (Lauder and Spalding, 1974).

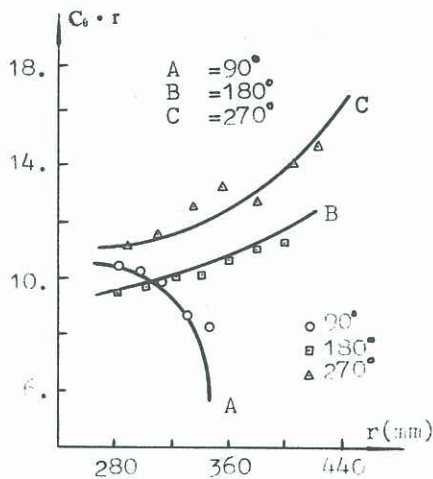


Fig.7 Angular momentum profiles ($z=0$)

Fig. 7 shows the distributions of the angular momentum ($C_\theta \cdot r$) in the symmetrical plane at the different θ . The distributions of the radial velocity in symmetrical plane at the different θ are shown in Fig. 8. The comparisons are made between the numerical results and the experimental data which were measured with the spherical five-hole probe. It is shown that agreement is satisfactory.

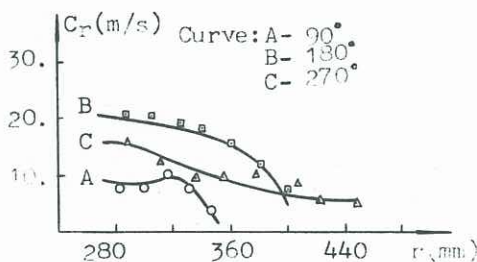


Fig.8 Radial velocity profiles ($z=0$)

Conclusions

The calculation procedure has been developed to predict the three-dimensional turbulent flow in general curvilinear

coordinates. Through the numerical study on the laminar entrance in a square duct, it is proved that the convergency and the precision of the present procedure are satisfactory. The turbulent flows are numerically calculated in a radial rotating duct and a volute with trapezoid cross-section. The predictions show physical realism and exhibit satisfactory agreement with the experimental results.

References

- Caretto, L. S., Gosman, A. D., Patankar, S. V., and Spalding, D. B., (1972). Two Calculation Procedure for Steady, Three-Dimensional Flows with Recirculation. *Proceedings of the Third International Conference on Numerical Methods in Fluid Dynamics*, Springer-Verlag, pp. 60-68.
- Demirdzic, I., Gosman, A. D., and Issa, R. I., (1980). A Finite-Volume Method for the Prediction of Turbulent Flow in Arbitrary Geometries. *Paper presented at 7th International Conference on Numerical Methods in Fluid Dynamics*, Stanford University and NASA Ames, June.
- Howard, J. H. G., Patankar, S. V., and Bordinuik, R. M., (1980). Flow Prediction in Rotating Ducts Using Coriolis-Modified Turbulence Models. *ASME Journal of Fluids Engineering*, Vol. 102, No. 4, pp. 456-462.
- Lauder, B. E. and Spalding, D. B., (1974). The Numerical Calculation of Turbulent Flows. *Computer Methods in Applied Mechanics and Engineering*. Vol. 3, No. 2, pp. 269-289.
- Neti, S. and Eichhorn, R., (1983). Combined Hydrodynamic and Thermal Development in a Square Duct. *Numerical Heat Transfer*, Vol. 6, pp.497-510
- Patankar, S. V., (1980) *Numerical Heat Transfer and Fluid Flow*, McGraw-Hill.
- Rhie C. M. and Chow, W. L., (1983). Numerical Study of the Turbulent Flow Past an Airfoil with Trailing Edge Separation. *AIAA Journal*, Vol. 21, No. 14, pp 1525-1532
- Song Baojun, (1990). Effects of Curvature and Rotation on Internal Three-Dimensional Turbulent Flows by Method of Modified $k-\epsilon$ Turbulence Model, Ph. D. Thesis, Xi'an Jiaotong University, P. R. China.
- Wagner, R. M. and Velkoff, H. R., (1972). Measurement of Secondary Flow in a Rotating Duct. *ASME Journal of Engineering for Power*, Vol. 94, pp 261-270